

**Linking RESRAD-OFFSITE and HYDROGEOCHEM Model for Performance Assessment of Low-Level Radioactive Waste Disposal Facility – 13429**

Wen-Sheng Lin\*, Charley Yu\*\*, Jing-Jy Cheng\*\*, Sunita Kamboj\*\*, Emmanuel Gnanapragasam\*\*, Chen-Wuing Liu\*\*\*, Ming-Hsu Li\*\*\*\*

† Hydrotech Research Institute, National Taiwan University, Taiwan

‡ Argonne National Laboratory, Argonne, IL 60439

§ Department of Bioenvironmental Systems Engineering, National Taiwan University, Taiwan

¶ Institute of Hydrological and Oceanic Sciences, National Central University, Taiwan

**ABSTRACT**

Performance assessments are crucial steps for the long-term radiological safety requirements of low-level waste (LLW) disposal facility. How much concentration of radionuclides released from the near-field to biosphere and what radiation exposure levels of an individual can influence on the satisfactory performance of the LLW disposal facility and safety disposal environment. Performance assessment methodology for the radioactive waste disposal consists of the reactive transport modeling of safety-concerned radionuclides released from the near-field to the far-field, and the potential exposure pathways and the movements of radionuclides through the geosphere, biosphere and man of which the accompanying dose. Therefore, the integration of hydrogeochemical transport model and dose assessment code, HYDROGEOCHEM code and RESRAD family of codes is imperative. The RESRAD family of codes such as RESRAD-OFFSITE computer code can evaluate the radiological dose and excess cancer risk to an individual who is exposed while located within or outside the area of initial (primary) contamination. The HYDROGEOCHEM is a 3-D numerical model of fluid flow, thermal, hydrologic transport, and biogeochemical kinetic and equilibrium reactions in saturated and unsaturated media. The HYDROGEOCHEM model can also simulate the crucial geochemical mechanism, such as the effect of redox processes on the adsorption/desorption, hydrogeochemical influences on concrete degradation, adsorption/desorption of radionuclides (i.e., surface complexation model) between solid and liquid phase in geochemically dynamic environments. To investigate the safety assessment of LLW disposal facility, linking RESRAD-OFFSITE and HYDROGEOCHEM model can provide detailed tools of confidence in the protectiveness of the human health and environmental impact for safety assessment of LLW disposal facility.

**INTRODUCTION**

The engineered barriers system (EBS) is an integral part of the radioactive waste disposal facility. The EBS represents the manmade, engineered materials of a repository, including the waste form,

waste canisters, concrete barrier, buffer materials, backfill, and seals, and can be used as physical and/or chemical obstructions to prevent or hinder the migration of radionuclides [1]. Several current disposal concepts indicate that concrete is an effective confinement material that is used in engineered barriers at a number of low-level radioactive waste (LLW) disposal sites in most countries [1, 2]. However, the lack of an appropriate EBS design in the concrete barrier, backfill, and the selection of sealing and covering materials for trenches, vaults, and ditches may result in the ingress of groundwater and the release of radionuclides from the disposed wastes to the biosphere [1-3]. The hydrogeochemical environment of an LLW repository is determined by the composition of groundwater and mineral formation, which may influence the chemical compatibility of backfill material, the concrete barrier, and the buffer material in the near field. The repository environment (for example, the pH, Eh, and ionic composition of the surrounding water) can affect EBS performance in waste storage and disposal. A number of reactions may occur simultaneously in groundwater and cement-based materials, including the dissolution of portlandite that is generated from the intrusion of hydrogen ion, increase of the concentration of calcium in the pore solution, formation of ettringite by sulfate attacking the cement, and dissolution of Calcium-Silicate-Hydrate (CSH) gel by chloride entering the cement, and the formation of Friedel's salt [4-6]. Bruno et al. [7] indicated that the interaction of pore water with accessory minerals of bentonite, such as sulfate dissolution-precipitation, and pyrite oxidation controlled the geochemical characteristics of the system. Therefore, the durability of cementitious material in service environments has presented a number of concerns, such as whether the EBS may be completely isolated from the groundwater, the hydrogeochemical reactions and key aqueous species in the groundwater that affect the degradation of the concrete barrier of the repository, and the influence of the redox processes on the formations of degradation materials. To obtain further insights into these interactions and provide a detailed overview of the long-term evolution in the hydrogeochemical environment of the concrete barrier, reactive chemical transport model can assess the hydrogeochemical influences on concrete barrier degradation.

In the past, groundwater and radionuclide transport calculations for performances assessment of a LLW often asked empirical approaches such as the linear isotherm ( $K_d$  approach) to handle the heterogeneous interphase reactions [8-15]. A distribution coefficient ( $K_d$ ) can describe the heterogeneous interphase behavior of radionuclide on a particular solid phase at a specific pH, Eh, and ionic composition of the surrounding water, but under variable environmental conditions the  $K_d$  approach cannot predict the behavior of radionuclide in geochemically dynamic environments. Surface complexation model can account for changes in ionic composition of water chemistry and mineralogy as a function of time and their effects on radionuclide geochemical transport [12]. Reactive chemical transport model incorporates the surface complexation reactions can also provide a much more powerful basis for assessing the radionuclide reactive transport from the near-field to the far-field.

However, performance assessment(PA) methodology for the radioactive waste disposal not only simulates the hydrogeochemical transport of concerned radionuclides released from engineered barriers system (EBS) to far-field, but must also consider the potential exposure pathways and the movements of radionuclides through the biosphere to man of which the accompanying dose. Therefore, the link of hydrogeochemical transport model and dose assessment code, HYDROGEOCHEM code and RESRAD family of codes could gain further insights into these PA problems. The RESRAD-OFFSITE computer code can evaluate the radiological dose and excess cancer risk to an individual who is exposed while located within or outside the area of initial (primary) contamination [16]. To investigate the safety assessment of LLW disposal facility, the three-dimensional groundwater flow and reactive transport model, HYDROGEOCHEM, has linked with RESRAD-OFFSITE code. This study results can provide detailed tools of confidence in the protectiveness of the human health and environmental impact for safety assessment of low-level radioactive waste disposal facility.

#### **METHODOLOGY OF LINKING RESRAD-OFFSITE AND HYDROGEOCHEM**

RESRAD-OFFSITE is an extension of the RESRAD (onsite) computer code that was developed to estimate the radiological consequences to a receptor located onsite or outside the area of primary contamination. The partitioning of nuclides between the aqueous and solid phases is characterized by the equilibrium distribution coefficient ( $K_d$ ). It calculates radiological dose and excess lifetime cancer risk with the predicted radionuclide concentrations in the environment, and derives soil cleanup guidelines corresponding to a specified dose limit. The primary contamination, which is the source of all the releases modeled by the code, is assumed to be a layer of soil. The releases of contaminants from the primary contamination to the atmosphere, to surface runoff, and to groundwater are considered. The code models the movement of the contaminants from the primary contamination to agricultural areas, pastures, a dwelling area, a well, and a surface water body. It also models the accumulation of the contaminants at those locations where appropriate. Any contribution of the contaminants from the water sources to the land-based locations is also modeled. Nine exposure pathways are considered in RESRAD-OFFSITE: direct exposure from contamination in soil, inhalation of particulates, inhalation of radon, ingestion of plant food (i.e., vegetables, grain, and fruits), ingestion of meat, ingestion of milk, ingestion of aquatic foods, ingestion of water, and ingestion (incidental) of soil.[16]

In a LLW geological repository, EBS is designed to prevent groundwater from contacting the canisters, cement-solidified waste forms and radionuclides in the container. In the case of EBS failure, the ingress of groundwater may cause the redox condition evolution in the near-field and chemical reactions between water and waste disposal facility, and result in canister metal corrosion, concrete barrier degradation and radionuclide dissolution. Radionuclides can eventually be released from the disposed wastes and migrate through the EBS to the biosphere.

RESRAD-OFFSITE cannot simulate the three-dimensional variably saturated-unsaturated groundwater flow, heat transfer and reactive biogeochemical transport, and the crucial hydrogeochemical mechanism, such as hydrogeochemical influences on concrete degradation, the effect of adsorption/desorption (i.e., surface complexation model) between radionuclides and geomedias on the transport behavior of radionuclides in geochemically dynamic environments. However, one of the most powerful features of RESRAD-OFFSITE is the ability to link a more sophisticated model that specifies the radionuclides source characteristics and release to the code. The feature of overriding the RESRAD-OFFSITE source term model can allow the reactive transport model, HYDROGEOCHEM, to link the RESRAD-OFFSITE, and simulate the hydrogeochemical transport and dose assessment of radionuclides for performance assessment of LLW disposal facility.

As mentioned above, the RESRAD-OFFSITE computational code can be flagged to suppress its source term module and to read in the time series of the information to the groundwater pathway. The name of the file containing the temporal source term and release data and their contents is described in Table 1.

TABLE I. Input file used to specify the source characteristics and releases to the code

File name	Contents
AQFLUXIN.DAT	Temporal data of the flux, in pCi year <sup>-1</sup> , of each initially present radionuclide and its principal nuclide progeny, to the groundwater pathway.

The data file is structured on the basis of the number of parent progeny combinations at the site. They contain a column of data for each parent-progeny combination. The order of the columns is determined as follows. The initially present nuclides are sorted first alphabetically by their chemical symbol and then by the nominal atomic weight in the case of isotopes. The first column of data pertains to the first nuclide in the sorted list. If that nuclide has principal radionuclide progeny, there must be a column of data for each progeny in the order in which they occur in the transformation chain. If the nuclide has more than one transformation thread, there must be additional columns of data for each transformation thread. Then there must be a column of data for the second initially present radionuclide in the sorted list, followed by a column each for its progeny in the order in which they occur in its transformation chain, and so on for each nuclide in the sorted list. The number of times at which data are available determines the number of rows in the different files — there must be a row for each time at which data are available. The computational code uses a linear interpolation between the specified times when performing the calculations. The input interface does not at present have a form to bypass the source module and accept these inputs because of the complexity of the format required for these input files. [16]

Regarding the HYDROGEOCHEM, the computer program developed by Yeh et al. [17], is a 3-D numerical model of fluid flow, thermal, hydrologic transport, and biogeochemical kinetic

and equilibrium reactions in saturated and unsaturated media. The latest version of HYDROGEOCHEM5.0 was designed for generic applications to reactive transport problems that are controlled by both kinetic and equilibrium reactions (e.g., aqueous complexation, precipitation-dissolution, adsorption/desorption, ion-exchange, redox, and acid-base reactions) in subsurface media. The effect of precipitation and dissolution on the change of pore size, hydraulic conductivity, and diffusion/dispersion were also incorporated. The flow equations, chemical transport equations, chemical equilibrium equations, initial boundary conditions, and numerical methods of the model are described in HYDROGEOCHEM5.0 manual [17]. The chemical transport equation of HYDROGEOCHEM model for linking the RESRAD-OFFSITE code is summarized as follows.

The governing equations for transport were derived based on the continuity of mass and Fick's flux laws. The main transport processes are advection, dispersion/diffusion, source/sink, and biogeochemical reactions (including radioactive decay). The general transport equation governing the temporal-spatial distribution of any biogeochemical species in a reactive system is described below. Let  $C_i$  be the concentration of the  $i$ -th species, the governing equation for  $C_i$  is obtained by applying the principle of mass balance in integral form as follows:

$$\frac{\partial \theta C_i}{\partial t} + \theta \alpha' \frac{\partial h}{\partial t} C_i = L(C_i) + \theta r_i + M_i, \quad i \in \{M\} \quad (\text{Eq. 1})$$

where  $L$  is the transport operator denoting

$$L(C_i) = -\nabla \cdot (\mathbf{V}C_i) + \nabla \cdot [\theta \mathbf{D} \cdot \nabla C_i] \quad (\text{Eq. 2})$$

where  $C_i$  is the concentration of the  $i$ -th species in units of chemical mass per water volume [ $M/L^3$ ];  $r_i$  is the production rate of the  $i$ -th species because of biogeochemical reactions in chemical mass per water volume per unit time [ $M/L^3/T$ ];  $\{M\} = \{1, 2, \dots, M\}$  in which  $M$  is the number of biogeochemical species;  $\mathbf{D}$  is the dispersion coefficient tensor [ $L^2/T$ ]; and  $M_i$  is the source/sink (other than sources because of chemical reactions) of the  $i$ -th species in chemical mass per unit volume of media [ $M/L^3/T$ ]. Four types of boundary conditions (Dirichlet, Cauchy, Neumann, and variable inflow-outflow) were implemented in HYDROGEOCHEM. The flux of advection and dispersion terms of aqueous radionuclides in the chemical transport equation is given by Equation 2. The temporal flux data of aqueous radionuclides released from the HYDROGEOCHEM simulated domain can be as the input data file of AQFLUXIN.DAT to the groundwater pathway in RESRAD-OFFSITE. Figure 1 shows that the schematic illustration of linking RESRAD-OFFSITE and HYDROGEOCHEM model. RESRAD-OFFSITE code considers three types of releases that lead to the contamination of the offsite locations. HYDROGEOCHEM can simulate the EBS degradation and radionuclides release from EBS to far field. The temporal flux data of radionuclides can be the input data file of AQFLUXIN.DAT

to the groundwater pathway in RESRAD-OFFSITE. A dust release-equilibrium model is used for the atmospheric release. The material that is eroded by surface runoff is modeled as a release to the surface water body. The atmospheric and runoff releases are effective once the surface soil layer becomes contaminated. Accumulation of radionuclides at the offsite locations is considered through deposition and irrigation.

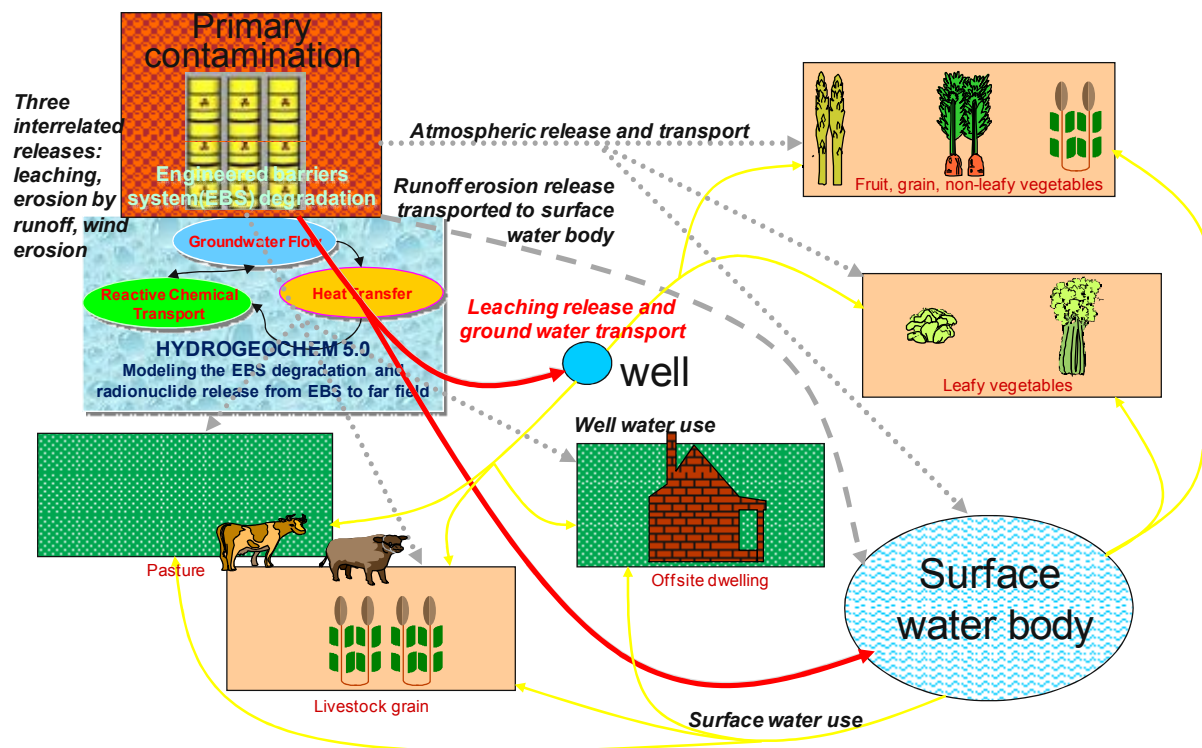


Fig. 1. Schematic illustration of linking RESRAD-OFFSITE and HYDROGEOCHEM model

### CASE STUDY OF LINKING MODEL

A potential site for the final disposal of LLW with a mined cavern design below the surface is proposed in Taiwan [18]. Concrete is an effective confinement material that is used in EBS. The case study of linking RESRAD-OFFSITE and HYDROGEOCHEM model is based on the EBS of the mined cavern design. The layout of the hypothetical site is depicted in Figure 2. The EBS is assumed to be the primary contamination in RESRAD-OFFSITE. Preliminary data gathered for this hypothetical site are as given below. The average annual precipitation at this location is 1.25 m/year. The primary contamination is not cultivated and is not irrigated. The cover management factor for the primary contamination is 0.04 and the runoff coefficient is 0.5. The leaf vegetable plot has a support practice factor of 0.9, a cover and management factor of 0.08 and a slope length steepness factor of 4. The fruit, grain non-leafy vegetable and livestock feed

grain are grown in relatively flat land. The cover management factor is 0.04. The ground level of the life stock feed grain growing area is 15 m above the ground level at the location of primary contamination. The corresponding differences in elevation for the leafy vegetable growing area and the dwelling site are 20 and 40 meters. All the other offsite location are at approximately the same elevation as the ground in the vicinity of the primary contamination. The hydraulic gradient of the groundwater is 0.053 across the entire site and the hydraulic conductivity is  $3.24 \times 10^{-8}$  m/s. The longitudinal, horizontal lateral and vertical lateral dispersivities to the surface waterbody are estimated to be 8, 0.8 and 0.05m respectively. The surface waterbody is the source of all water used in this scenario. For groundwater transport purposes, the surface water is 290 m along the groundwater flow line, from the down gradient edge of the primary contamination. The right and left edges of the surface waterbody are at 200 and 100 m from the groundwater flowline through the center of the primary contamination. The individual spends 0.5 of the time inside the dwelling, 0.2 of the time outdoors in the vicinity of the dwelling, 0.08 of the time in each of the vegetable plots and in the livestock grain field, and 0.01 of the time in the pasture. The remainder of time is spent away from the area. All other inputs are assumed to be at the pre-loaded RESRAD-OFFSITE value for this site analysis.

Figure 3 schematically illustrates the design of an engineered barrier. The thickness of the concrete barrier ranges from 0.5 m to 1.0 m. The inner and outer thicknesses of the bentonite buffer are 0.5 m and 0.2 m, respectively [18]. The safety-concerned radionuclide, I-129 was selected in the case study. Radionuclide anticipated activity of operating and decommissioning LLW contained in about 998,000 fifty-gallon drums is shown in Table II. The radioactive waste container types are carbon steel drum or galvanized steel drums. Steel corrosion caused by the oxidation or chemical reaction with the cementitious environments is expected to induce the container degradation eventually. What has to be noticed is containers will fail, thereby, exposing the radionuclide bundles to groundwater. Thus, the containers are assumed to last for 100 years. After 100 years of simulation time, the radionuclide would be uniformly released from waste container for a period of 100 years. The simulation region was discretized with 3,918 elements and 4,146 nodes for the EBS in HYDROGEOCHEM as illustrated in Figure 4. The vertical front edge, back edge, and horizontal top edge depict a no-flow boundary, except for the side ditch in the vertical front edge. The side ditch area on the front edge was set to a variable boundary condition, which is usually an air-media interface in which water uninterruptedly seeps out. The flux in the bottom edge caused by gravity was considered a Neumann boundary with a zero flux. The horizontal left and right edges were Dirichlet head-boundary conditions. The total head on the horizontal left and right edge nodes were assumed as 432.8 dm and 420 dm, respectively. As the repository starts to operate, the EBS will expose to groundwater and the cementitious materials of concrete will interact with groundwater. To mitigate this type interaction, it is important to avoid the concrete immersion by the inflow of groundwater. Therefore, the side ditch system is designed at the bottom of the disposal tunnel and allows the

drainage of water. If the groundwater inflow is drained from the side ditch, the effect of concrete degradation on performance of EBS may be reduced [18]. Hence, simulation scenarios considered in HYDROGEOCHEM are the PA of EBS and radionuclide release with side ditch.

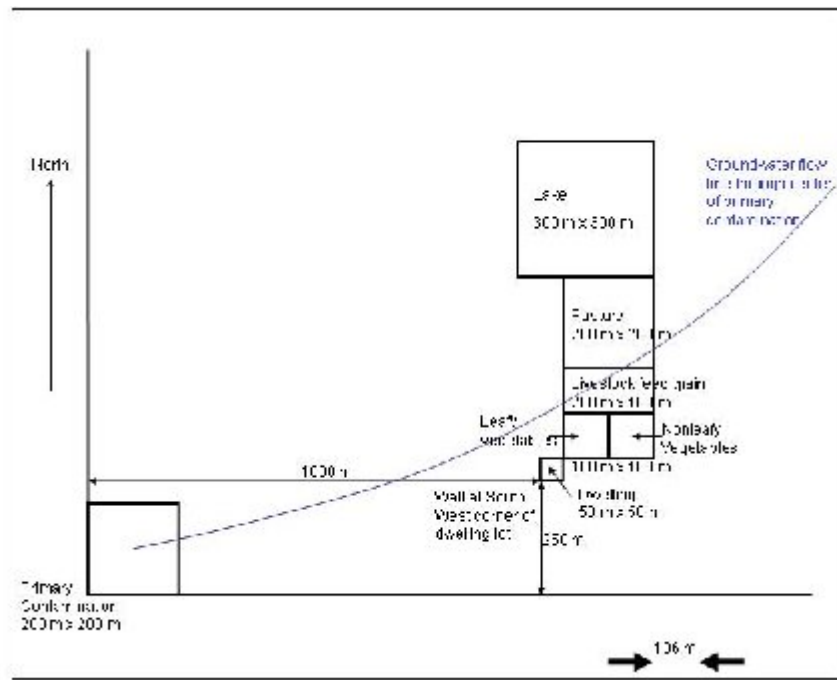


Fig. 2. The layout of the hypothetical site

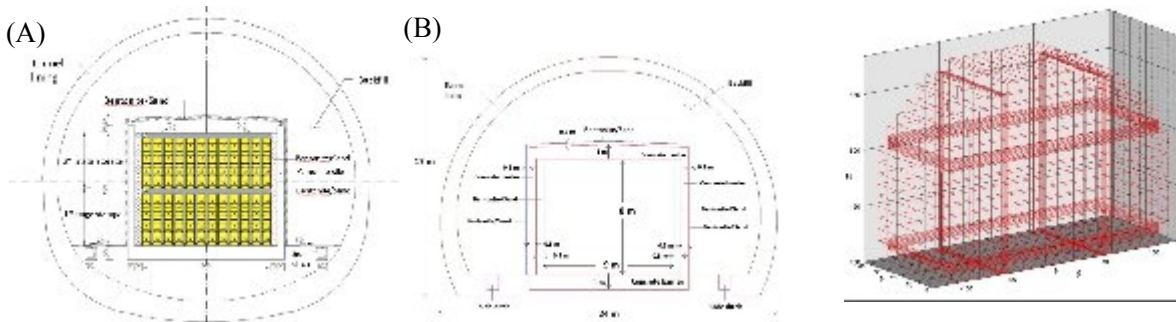


Fig. 3. Schematic illustration of the EBS design: (A) Cross-section of the tunnel (B) Conceptual model for the cross-section of the tunnel.

Fig. 4. Numerical discretization of grids for HYDROGEOCHEM.

Table II The half-life and activity for the safety- concerned radionuclides.

Radionuclide	Half-life (years)	Activity (Bq)	Concentration(mole/l)
I-129	$1.57 \times 10^7$	$4.48 \times 10^{11}$	$5.42 \times 10^{-10}$

Table III provides a summary of the physical parameters for groundwater flow and the reactive transport simulations. Table IV presents the initial and boundary conditions, and other



parameters that were used in HYDROGEOCHEM. The study considered the hydrogeochemical transport of 15 components, including  $\text{Na}^+$ ,  $\text{K}^+$ ,  $\text{Ca}^{2+}$ ,  $\text{Al}^{3+}$ ,  $\text{OH}^-$ ,  $\text{HCO}_3^-$ ,  $\text{Cl}^-$ ,  $\text{SO}_4^{2-}$ ,  $\text{H}_4\text{SiO}_4$ ,  $\text{Fe}^{3+}$ ,  $e^-$ ,  $\Gamma^-$ ,  $>\text{S}_{\text{Al}}\text{OH}$  and  $>\text{S}_{\text{Fe}}\text{OH}$ , 37 aqueous species, 2 solid-phase radionuclides of precipitation/dissolution reactions, 10 minerals of precipitation/dissolution reactions, and 6 adsorbed species. Table V-VIII list the thermodynamic data of reactions (e.g., precipitation-dissolution, adsorption-desorption, and aqueous complexation) considered in HYDROGEOCHEM. The surface complexation model (e.g., triple-layer model) was used to describe sorption of I-129 on the aluminium oxide and ferric oxide surface of cement mineral. The adsorbent components,  $>\text{S}_{\text{Al}}\text{OH}$  and  $>\text{S}_{\text{Fe}}\text{OH}$ , was specified as sorbing site of aluminium oxide and ferric oxide surface, respectively. The simulation time in HYDROGEOCHEM was 1000 years with an initial time-step of  $1.0 \times 10^{-5}$  year, and a maximal allowable time-step of 0.01 year.

Table III Physical parameters used in HYDROGEOCHEM 5.0 model.

Media	K (m/s)	Porosity (%)	Diffusion coefficient (m <sup>2</sup> /s)	Bulk density (kg/m <sup>3</sup> )	Longitudinal dispersivity (m)	Lateral dispersivity (m)
Cement-solidified waste canister	$8.70 \times 10^{-9}$	0.15	$3.0 \times 10^{-12}$	1200	0.1	0.01
Concrete	$3.1 \times 10^{-14}$	0.15	$3.0 \times 10^{-12}$	2030	0.10	0.010
Bentonite	$5.0 \times 10^{-11}$	0.363	$1.2 \times 10^{-10}$	2000	0.15	0.015
Backfill	$3.24 \times 10^{-8}$	0.168	$2.0 \times 10^{-11}$	2410	0.30	0.030

Table IV Initial and boundary conditions used in HYDROGEOCHEM.

Component	Initial Conditions				Boundary Conditions
	Concrete	Bentonite	Backfill	Cement-solidified waste form	Groundwater
$\text{Na}^+$	$6.908 \times 10^{-2}$	$1.69 \times 10^{-1}$	$1.01 \times 10^{-4}$	$1.50 \times 10^{-2}$	$7.68 \times 10^{-5}$
$\text{K}^+$	0.2665	$1.14 \times 10^{-3}$	$1.84 \times 10^{-6}$	$8.90 \times 10^{-2}$	$1.84 \times 10^{-6}$
$\text{Ca}^{2+}$	29.906	$9.97 \times 10^{-3}$	$3.61 \times 10^{-2}$	15.46	$3.21 \times 10^{-2}$
$\text{Al}^{3+}$	2.628	$1.00 \times 10^{-20}$	$3.33 \times 10^{-14}$	$5.16 \times 10^{-1}$	$2.71 \times 10^{-8}$
$\text{OH}^-$	21.1	$1.91 \times 10^{-7}$	$3.43 \times 10^{-7}$	7.75	$3.43 \times 10^{-7}$
$\text{HCO}_3^-$	$1.394 \times 10^{-11}$	$2.14 \times 10^{-3}$	$3.60 \times 10^{-4}$	$1.22 \times 10^{-1}$	$3.81 \times 10^{-4}$
$\text{Cl}^-$	$5.64 \times 10^{-5}$	$1.53 \times 10^{-1}$	$1.79 \times 10^{-4}$	$3.80 \times 10^{-2}$	$1.58 \times 10^{-4}$
$\text{SO}_4^{2-}$	$1.633 \times 10^{-3}$	$2.94 \times 10^{-2}$	$8.57 \times 10^{-2}$	$1.633 \times 10^{-3}$	$8.81 \times 10^{-2}$
$\text{H}_4\text{SiO}_4$	9.198	$6.60 \times 10^{-5}$	$1.51 \times 10^{-4}$	$4.72 \times 10^{-3}$	$1.51 \times 10^{-4}$
$\text{Fe}^{3+}$	$3.10 \times 10^{-2}$	$1.0 \times 10^{-8}$	$1.0 \times 10^{-10}$	$3.1 \times 10^{-2}$	$8.79 \times 10^{-4}$
pe	-1.0	-0.70	-1.0	-1.0	-1.0

Table V Precipitation-dissolution reactions of solid-phase radionuclides considered in the HYDROGEOCHEM 5.0 model.

Precipitation-dissolution reactions of solid-phase radionuclide (25°C)					
No.	Reaction	log K	No.	Reaction	log K
1	$\text{Ca}^{2+} + 2\text{I}^- + 12\text{OH}^- = \text{Ca}(\text{IO}_3)_2(\text{s}) + 12\text{e}^- + 6\text{H}_2\text{O}$	-45.07	2	$2\text{I}^- = \text{I}_{2(\text{s})} + 2\text{e}^-$	-18.30

Table VI Precipitation-dissolution reactions of mineral considered in the HYDROGEOCHEM 5.0 model.

Precipitation-dissolution reactions of mineral (25°C)				
No.	Mineral	Reaction	log K	Molar volume (dm <sup>3</sup> /mole)
1	Calcite	$\text{HCO}_3^- + \text{Ca}^{2+} + \text{OH}^- = \text{CaCO}_3 + \text{H}_2\text{O}$	12.151	0.03693
2	Portlandite	$\text{Ca}^{2+} + 2\text{OH}^- = \text{Ca}(\text{OH})_2$	5.20	0.03300
3	Ettringite	$2\text{Al}^{3+} + 6\text{Ca}^{2+} + 26\text{H}_2\text{O} + 3\text{SO}_4^{2-} + 12\text{OH}^- = \text{Ca}_6\text{Al}_2(\text{SO}_4)_3(\text{OH})_{12} \cdot 26\text{H}_2\text{O}$	111.03	0.71032
4	Quartz	$\text{H}_4\text{SiO}_4 = \text{SiO}_2 + 2\text{H}_2\text{O}$	3.98	0.02269
5	Gypsum	$\text{Ca}^{2+} + \text{SO}_4^{2-} + 2\text{H}_2\text{O} = \text{CaSO}_4 \cdot 2\text{H}_2\text{O}$	4.58	0.07470
6	Hydrogarnet	$2\text{Al}^{3+} + 3\text{Ca}^{2+} + 12\text{OH}^- = \text{Ca}_3\text{Al}_2(\text{OH})_{12}$	87.68	0.14952
7	Friedel's salt	$2\text{Al}^{3+} + 4\text{Ca}^{2+} + 2\text{Cl}^- + 4\text{H}_2\text{O} + 12\text{OH}^- = 2\text{Ca}_2\text{Al}(\text{OH})_6\text{Cl} \cdot 2\text{H}_2\text{O}$	93.07	0.27624
8	Thaumasite	$3\text{Ca}^{2+} + \text{H}_4\text{SiO}_4 + \text{SO}_4^{2-} + \text{HCO}_3^- + 11\text{H}_2\text{O} + 3\text{OH}^- = \text{Ca}_3\text{SiO}_3 \cdot \text{CaSO}_4 \cdot \text{CaCO}_3 \cdot 15\text{H}_2\text{O}$	31.70	0.32940
9	Monocarboaluminate	$2\text{Al}^{3+} + \text{HCO}_3^- + 4\text{Ca}^{2+} + 3.68\text{H}_2\text{O} + 13\text{OH}^- = 3\text{CaO} \cdot \text{Al}_2\text{O}_3 \cdot \text{CaCO}_3 \cdot 10.68\text{H}_2\text{O}$	101.45	0.26196
10	Pyrite	$\text{FeS}_2 + 2\text{H}^+ + 2\text{e}^- = \text{Fe}^{2+} + 2\text{HS}^-$	-18.479	0.02394

Table VII Adsorption-desorption reactions considered in the HYDROGEOCHEM 5.0 model.[19]

Adsorption-Desorption Reactions (25°C)					
No.	Reaction	log K	No.	Reaction	log K
1	$>\text{S}_{\text{Al}}\text{OH}_2^+ + \text{IO}_3^- = >\text{S}_{\text{Al}}\text{OH}_2^+ \cdot \text{IO}_3^-$	4.3	4	$>\text{S}_{\text{Fe}}\text{OH}_2^+ + \text{IO}_3^- = >\text{S}_{\text{Fe}}\text{OH}_2^+ \cdot \text{IO}_3^-$	4.6
2	$2>\text{S}_{\text{Al}}\text{OH}_2^+ + \text{IO}_3^- = >\text{S}_{\text{Al}}\text{OH}_2^+ \cdot \text{IO}_3^- + 2\text{H}_2\text{O}$	9.1	5	$2>\text{S}_{\text{Fe}}\text{OH}_2^+ + \text{IO}_3^- = >\text{S}_{\text{Fe}}\text{OH}_2^+ \cdot \text{IO}_3^- + 2\text{H}_2\text{O}$	9.9
3	$>\text{S}_{\text{Al}}\text{OH} + \text{H}^+ = >\text{S}_{\text{Al}}\text{OH}_2^+$	4.5	6	$>\text{S}_{\text{Fe}}\text{OH} + \text{H}^+ = >\text{S}_{\text{Fe}}\text{OH}_2^+$	6.3

Table VIII Aqueous complexation reactions considered in the HYDROGEOCHEM 5.0 model.

Aqueous complexation reactions (25°C)					
No.	Reaction	log K	No.	Reaction	log K
1	$\text{HCO}_3^- = \text{CO}_2(\text{aq}) + \text{OH}^-$	-7.648	20	$\text{Fe}^{3+} + \text{e}^- = \text{Fe}^{2+}$	13.02
2	$\text{HCO}_3^- + 8\text{e}^- + 6\text{H}_2\text{O} = \text{CH}_4(\text{aq}) + 9\text{OH}^-$	-95.258	21	$\text{Fe}^{3+} + 4\text{OH}^- = \text{Fe}(\text{OH})_4^-$	34.4
3	$4\text{OH}^- = \text{O}_2 + 2\text{H}_2\text{O} + 4\text{e}^-$	-30.08	22	$\text{K}^+ + \text{Cl}^- = \text{KCl}$	-0.5
4	$2\text{H}_2\text{O} + 2\text{e}^- = 2\text{OH}^- + \text{H}_2$	-31.15	23	$\text{K}^+ + \text{OH}^- = \text{KOH}$	-0.46
5	$\text{H}_2\text{O} = \text{OH}^- + \text{H}^+$	-14	24	$\text{K}^+ + \text{SO}_4^{2-} = \text{KSO}_4^-$	0.85
6	$\text{Al}^{3+} + \text{OH}^- + \text{H}_4\text{SiO}_4 = \text{AlH}_3\text{SiO}_4^{2+} + \text{H}_2\text{O}$	-16.38	25	$\text{Mg}^{2+} + \text{HCO}_3^- + \text{OH}^- = \text{MgCO}_3^+ + \text{H}_2\text{O}$	6.651
7	$\text{H}_4\text{SiO}_4 + 2\text{OH}^- = \text{H}_2\text{SiO}_4^{2-} + 2\text{H}_2\text{O}$	5	26	$\text{Mg}^{2+} + \text{OH}^- = \text{MgOH}^+$	2.56
8	$\text{Ca}^{2+} + \text{H}_4\text{SiO}_4 + \text{OH}^- = \text{CaH}_3\text{SiO}_4^+ + \text{H}_2\text{O}$	5.17	27	$\text{Na}^+ + \text{Cl}^- = \text{NaCl}$	-0.5
9	$\text{Mg}^{2+} + \text{H}_4\text{SiO}_4 + \text{OH}^- = \text{MgH}_3\text{SiO}_4^+ + \text{H}_2\text{O}$	5.42	28	$\text{Na}^+ + \text{HCO}_3^- + \text{OH}^- = \text{NaCO}_3^- + \text{H}_2\text{O}$	4.961
10	$\text{H}_4\text{SiO}_4 + \text{OH}^- = \text{H}_3\text{SiO}_4^- + \text{H}_2\text{O}$	4.17	29	$\text{Na}^+ + \text{OH}^- = \text{NaOH}$	-0.18
11	$\text{Na}^+ + \text{H}_4\text{SiO}_4 + \text{OH}^- = \text{NaH}_3\text{SiO}_4(\text{aq}) + \text{H}_2\text{O}$	5.99	30	$\text{Na}^+ + \text{SO}_4^{2-} = \text{NaSO}_4^-$	0.94
12	$\text{Al}^{3+} + 4\text{OH}^- = \text{Al}(\text{OH})_4^-$	33.3	31	$\text{SO}_4^{2-} + \text{H}_2\text{O} = \text{HSO}_4^- + \text{OH}^-$	-12.012
13	$\text{K}^+ + \text{Al}^{3+} + 4\text{OH}^- = \text{KAl}(\text{OH})_4$	31.78	32	$\text{SO}_4^{2-} + 8\text{e}^- + 4\text{H}_2\text{O} = \text{S}^{2-} + 8\text{OH}^-$	-91.268
14	$\text{Na}^+ + \text{Al}^{3+} + 4\text{OH}^- = \text{NaAl}(\text{OH})_4$	32.37	33	$\text{SO}_4^{2-} + 8\text{e}^- + 5\text{H}_2\text{O} = \text{HS}^- + 9\text{OH}^-$	-92.35
15	$\text{Ca}^{2+} + \text{Cl}^- = \text{CaCl}^+$	-0.29	34	$\text{SO}_4^{2-} + 6\text{H}_2\text{O} + 8\text{e}^- = \text{H}_2\text{S} + 10\text{OH}^-$	-99.356
16	$\text{Ca}^{2+} + \text{HCO}_3^- + \text{OH}^- = \text{CaCO}_3 + \text{H}_2\text{O}$	6.895	35	$\text{FeCO}_3 = \text{Fe}^{3+} + \text{HS}^- + \text{e}^-$	-23.82
17	$\text{Ca}^{2+} + \text{OH}^- = \text{CaOH}^+$	1.22	36	$\text{I}^- + 6\text{OH}^- = \text{IO}_3^- + 6\text{e}^- + 3\text{H}_2\text{O}$	-25.61
18	$\text{Ca}^{2+} + \text{SO}_4^{2-} = \text{CaSO}_4$	2.3	37	$\text{Ca}^{+2} + \text{I}^- = \text{CaI}^+$	0.14
19	$\text{HCO}_3^- + \text{OH}^- = \text{CO}_3^{2-} + \text{H}_2\text{O}$	3.671			

## RESULT AND DISCUSSION

The simulated results revealed notable differences of I-129 concentration distribution after 500 and 1000 years in the hydrogeochemical transport of EBS was approximately to  $1.00 \times 10^{-23}$  M and  $1.00 \times 10^{-19}$  M, respectively as shown in Figure 4. The mineral saturation index (SI) was much less than zero due to the low aqueous concentrations of radionuclide, so the precipitation of I-129 related minerals was not found in EBS. Figures 5(A) and 5(B) demonstrate that iodate( $\text{IO}_3^-$ ) was not formed. Thus, the adsorption behaviors of iodate( $\text{IO}_3^-$ ) by aluminium oxide and ferric oxide were not found. Nagata [14] pointed out the adsorption of iodate on naturally occurring oxides under occurring oxides under oxic conditions is of environmental concern. He also reported that aqueous iodine species occur mainly as iodide ( $\text{I}^-$ ) and iodate, depending on the redox conditions. Therefore, the redox processes markedly influence on the formations of the iodide and iodate.

Figure 6 is the schematic illustration of map interface for the hypothetical site in RESRAD-OFFSITE. The temporal flux data of aqueous I-129 released from the HYDROGEOCHEM simulated domain can be the input data file of AQFLUXIN.DAT to the groundwater pathway in RESRAD-OFFSITE. Figure 7 shows the total dose of I-129 from all pathways with a small amount of  $2.0 \times 10^{-19}$  mSv/year after 1000 years. This value is much less than the dose limit of 0.25 mSv/year to the individual expected to receive the greatest exposure to residual radioactivity

The study selected the safety-concerned I-129 radionuclide for linking RESRAD-OFFSITE and HYDROGEOCHEM model. However, the thermodynamic database used in reactive transport model should be expanded to include all the radionuclides (more than 830) contained in the International Commission on Radiological Protection (ICRP) 38 database for the performance assessment of low-level radioactive waste disposal facility in future study. Moreover, to simulate the whole subsurface system, the simulation region of HYDROGEOCHEM can be extended to the far-field to obtain further insights of radionuclides migration and reactive transport in the hydrogeochemical environment of geosphere.

The radioactive waste container materials are made from carbon steel, galvanized steel, stainless steel, other materials. Hydrogeochemical evolution of near-field can cause the oxidation or chemical reactions with the cementitious environments. Eventually, the steel corrosion is expected to induce the container degradation. Thus, it must be noted that containers will fail, thereby, exposing the radionuclide to groundwater. Kursten et al.[19] pointed out that the both uniform and localized corrosion are possible at various stages under repository conditions, depending on the precise physical and chemical environment surrounding the metallic container. He also reported that the most common forms of localised corrosion are pitting corrosion, crevice corrosion, stress corrosion cracking, and microbially influenced corrosion. Electrical

coupling with other metals can lead to accelerated corrosion, by a process known as galvanic coupling, and the presence of radiation fields can affect the corrosion behavior of metals by producing highly reactive species in-situ. Therefore, these possible degradation modes will be addressed in the reactive transport model in future study.

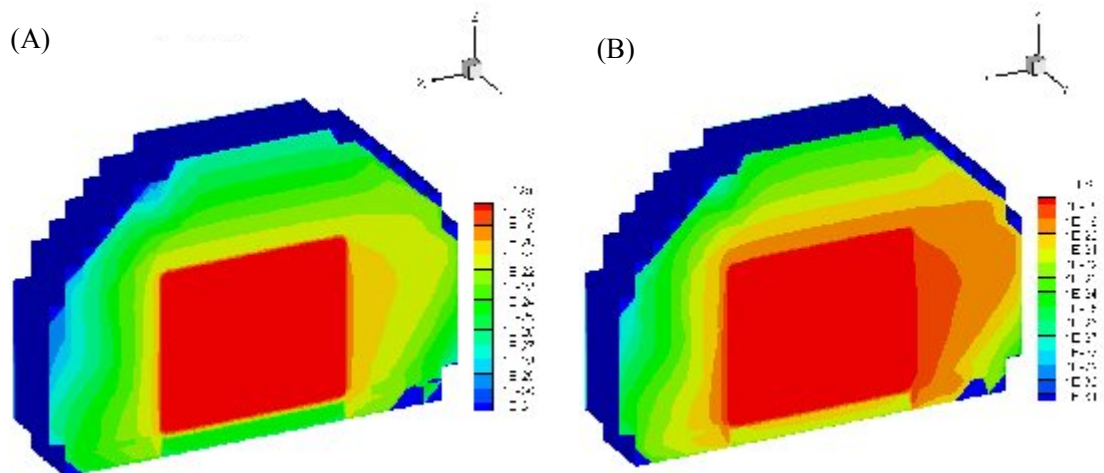


Fig. 4. Distribution of I-129 concentration (mole/l) in EBS: (A) after 500 years, (B) after 1000 years

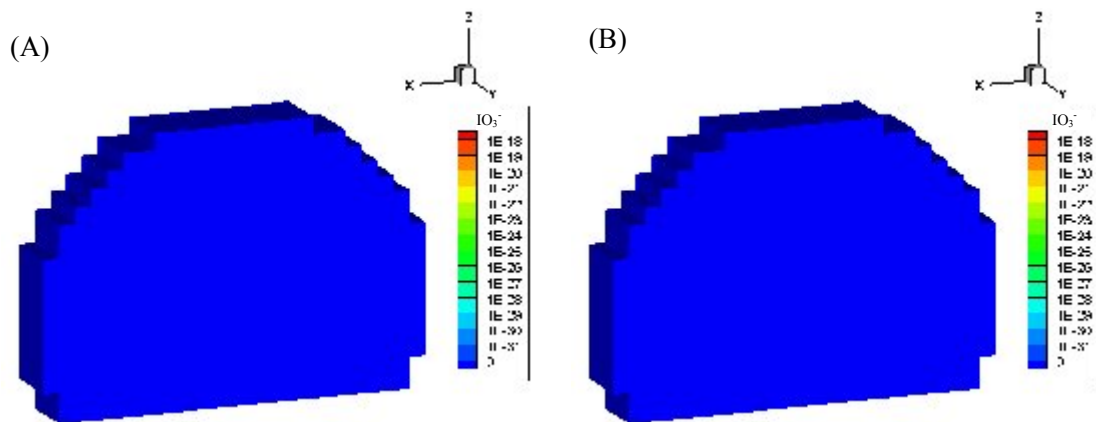


Fig. 5. Distribution of  $\text{IO}_3^-$  concentration (mole/l) in EBS: (A) after 500 years, (B) after 1000 years

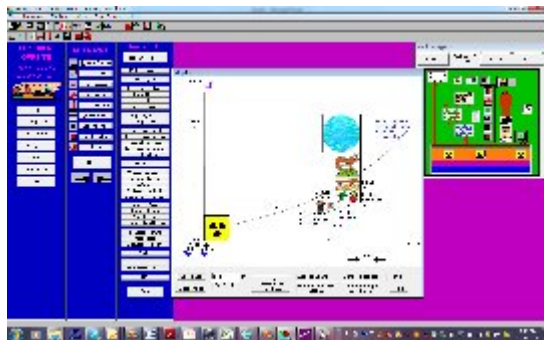


Fig. 6. Map interface of the hypothetical site in RESRAD-OFFSITE.

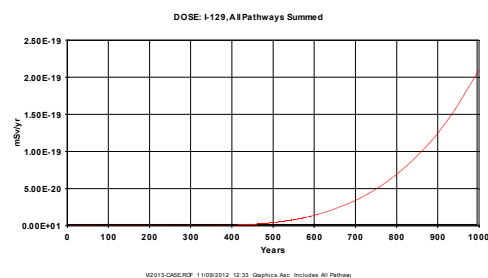


Fig. 7. Total dose of I-129 from all pathways.

### CONCLUSION AND SUGGESTION

Performance assessment methodology for the radioactive waste disposal not only simulates the hydrogeochemical transport of concerned radionuclides released from engineered barriers system (EBS) to far-field, but must also consider the potential exposure pathways and the movements of radionuclides through the biosphere to man of which the accompanying dose. The link of hydrogeochemical transport model and dose assessment code, HYDROGEOCHEM code and RESRAD family of codes could gain further insights into these PA problems. The redox processes markedly influence on the adsorption/desorption (i.e., surface complexation model) which could be a crucial geochemical mechanism for the modeling of liquid-solid phase behavior of radionuclide in geochemically varied environments. Moreover, steel corrosion is expected to induce the container degradation and these possible degradation modes will be addressed in the reactive transport model in the future study. The development of advanced numerical models that are coupled with hydrogeochemical transport and dose assessment of radionuclide is required in future research. The effective prediction tool of the advanced numerical models can provide confidence in the protection of the human and environmental health for PA of the EBS.

### ACKNOWLEDGEMENT

The authors are grateful to the National Science Council, Republic of China, for financial support of this research under contract No. NSC 101-2918-I-002-034, NSC 101-3113-E-007-008 and NSC 101-3113-E-002-006.

### REFERENCES

1. IAEA, *Performance of Engineered Barrier Materials in Near Surface Disposal Facilities for Radioactive Waste*, p.50, IAEA — TECDOC-1255, Vienna (2001).
2. IAEA, *Technical considerations in the design of near surface disposal facilities for radioactive waste*, p.53, IAEA — TECDOC-1256, Vienna (2001).
3. IAEA, *Near Surface Disposal of Radioactive Waste, IAEA Safety Standards Series, Requirements*, p.29,

- IAEA —WS-R-1, Vienna (1999).
4. C. JANTZEN, A. JOHNSON, D. READ AND J. A. STEGEMANN, “Cements in waste management”, *Advances in Cement Research*, **22**(4), 225 (2010).
  5. F.P. GLASSER, J. MARCHAND AND E. SAMSON, “Durability of concrete – Degradation phenomena involving detrimental chemical reactions”, *Cement and Concrete Research*, **38**, 226 (2008).
  6. M. LUNA, D. ARCOS, L. DURO, *Effects of grouting, shotcreting and concrete leachates on backfill geochemistry*, p51, Svensk Kärnbränslehantering AB, SKB R-06-107( 2006).
  7. J. BRUNO, D. ARCOS, L. DURO, *Processes and features affecting the near field hydrochemistry: Groundwater-bentonite interaction*, p56, Svensk Kärnbränslehantering AB, SKB TR-99-29 (1999).
  8. OCHS, M., POINTEAU, I., AND GIFFAUT, E., “Caesium sorption by hydrated cement as a function of degradation state: experiments and modelling”, *Waste Management*, **26** 725 (2006).
  9. SULLIVAN, T.M. *Disposal Unit Source Term (DUST) Data Input Guide*. Technical Report NUREG/CR6041, BNL-NUREG-52375, U. S. Nuclear Regulatory Commission, Washington, DC (1993).
  10. SULLIVAN, T.M. AND SUEN, C. J. *Low-Level Waste Shallow Land Disposal Source Term Model: Data Input Guides*, Technical Report NUREG/CR-5387, BNL-NUREG-52206, U. S. Nuclear Regulatory Commission, Washington, DC (1989).
  11. KOZAK, M.W., CHU, M S.Y., MATTINGLY, P.A., JOHNSON, J. D., AND MCCORD, J. T. *Background Information for the Development of a Low-Level Waste Performance Assessment Methodology - Computer Code Implementation and Assessment*, Technical Report NUREG/CR-5453, SAND90-0375, Vol. 5, U. S. Nuclear Regulatory Commission, Washington, DC (1990).
  12. ZAVARIN, M. AND BRUTON, C. J., *A Non-Electrostatic Surface Complexation Approach to Modeling Radionuclide Migration at the Nevada Test Site: Iron Oxides and Calcite*. Technical Report UCRL-TR-208673, Lawrence Livermore National Laboratory, Livermore, California (2004).
  13. MARMIER, N., DELISEE, A., FROMAGE, F., “Surface Complexation Modeling of Yb(III) and Cs(I) Sorption on Silica”. *Journal of Colloid and Interface Science*, **212**, 228(1999)
  14. NAGATA, T., FUKUSHI, K., “Prediction of iodate adsorption and surface speciation on oxides by surface complexation modeling”, *Geochimica et Cosmochimica Acta* , **74**, 6000 (2010).
  15. CARROLL, S.A., ROBERTS, S.K., CRISCENTI, L.J., O'DAY, P.A., “Surface complexation model for strontium sorption to amorphous silica and goethite”. *Geochemical Transactions*, **9**, 2 (2008)
  16. YU, C., et al., *User's Manual for RESRAD-OFFSITE Version 2*, ANL/EVS/TM/07-1, Argonne National Laboratory, Argonne, IL (2007).
  17. G. T. YEH, J. SUN, P. M. JARDINE, W. D. BURGOS, Y. FANG, M. H. LI AND M. D. SIEGEL, *HYDROGEOCHEM 5.0: A three-Dimensional model of coupled fluid flow, thermal transport, and hydrogeochemical transport through variably saturated conditions – version 5.0*, p. 243, ORNL/TM-2004/107, Oak Ridge National Laboratory, Oak Ridge, TN (2004).
  18. W.S. LIN, C.W. LIU, J.H. TSAO, and M.H. LI, “Modeling the Hydrogeochemical Transport of Radionuclides through Engineered Barriers System in the Proposed LLW Disposal Site of Taiwan-12082”, *WM2012 Conference*, Phoenix, AZ, February 26 - March 1 (2012).
  19. B. KURSTEN, E. SMAILOS, I.AZKARATE, L. WERME, N.R. SMART, AND G. SANTARINI, *COBECOMA (State-of-the-art document on the COrrOsion BEhaviour of Container Materials)*, Final report, EUROPEAN COMMISSION (2003).